BUK-2020
BAYERO UNIVERSITY, KANO-CONFERENCE 2020
The Proceeding of 19th Multi-disciplinary Academic Conference, Hummingbird Publications and Research International on Refocusing: Challenges and Opportunities in 21st Century. Vol. 21 No. 1, 30th July, 2020 at Baayero University, BUK, Old Side Campus, Kan

PHYTO-ENHANCED SYNTHESIS OF IRON OXIDE NANOPARTICLES USING AQUEOUS EXTRACT OF *CALOTROPIS PROCERA*

ASUQUO, UTIBE RIVENUS*, ISA, ABUBAKAR GARBA AND ABDULKAREEM, AMBALI SAKA
Department of Chemical Engineering, Federal University of Technology, Minna – Nigeria

Abstract
In this work, green synthesis of iron oxide nanoparticles with extract of Calotropis procera as reducing and capping agent was carried out. Fe^{3+}: Fe^{2+} were mixed in ration 2: 1 on mole ratio and the resulting mixture was adjusted to pH 9. The mixture of the salt precursor and the plant extract yielded an immediate colour change and was stirred for a period of 1 hour. The resulting colloid obtained was characterized to determine the formation of iron oxide nanoparticle, size, morphology, crystallinity and the bond present using dynamic light scattering (DLS), UV-vis spectroscopy, X-ray diffraction (XRD) and Raman spectroscopy respectively. DLS showed particles having an average size of 54 nm, UV-vis spectroscopy showed the characteristic optical extinction of magnetite nanoparticles with absorption peak of 404 nm. XRD confirmed the formation of Fe_3O_4 nanoparticles having an average crystallite size of 19.6 nm. The degree of graphitization studied by Raman spectroscopy revealed dominant structure conforming to magnetite nanoparticles at frequency of 668 cm^{-1}. The phytochemicals that aided the reduction and stabilization of the nanoparticles was confirmed by FTIR spectra. The results support the fabrication of nanomaterials having possible potential for application as drilling fluid additive via the green synthesis route.

Keywords: *Nanoparticles, magnetite, phytochemicals, green synthesis, Raman spectroscopy*

Introduction
Increasing prominence in nanotechnology has paved way for the synthesis of iron oxide nanoparticle with varying physical and chemical properties, having diverse application in smart fluids, biomedical sciences, environmental remediation and energy transformation (Beheshtkhoo *et al.*, 2018). Mandeep and Dimple (2018) identified nanoparticle as comprising submicron segments of molecules with nanoscale dimensions of organic or inorganic materials and having novel attributes

compared to that of bulk materials. These nanoparticles could be synthesized using top-down approach which involves production of nanoparticles by size reduction of bulk material using mechanical techniques such as machining and grinding or through bottom-up approach involving the growing of nanoparticles from simpler molecules in reaction precursors (Saif *et al.*, 2016). According to Mahmoud *et al.*, (2019), the diverse application of iron oxide nanoparticles (NPs) is attributed to their outstanding physicochemical properties, high catalytic activities and higher intrinsic reactivity. Campos *et al.*, (2015) proposed that particle size, more active sites and high surface area offer iron oxide nanoparticle enhance their catalytic effects during thermal oxidation reactions. Other advantages include its unique properties such as biocompatibility, biodegradability, paramagnetic and superparamagnetic effects (Yew *et al.*, 2016). Chemical methods such as co-precipitation, hydrothermal synthesis, polyol suspension, sol-gel, electrochemical reactions, sonochemical reactions, thermal decomposition and microemulsion methods are commonly employed in the synthesis of iron oxide nanoparticles.
However, the overwhelming complexity, high energy requirement, negative impacts of synthesis procedures, their accompanying chemicals and derivative compounds associated with the chemical methods used in the synthesis of iron oxide nanoparticles calls for attention. Thus, green synthesis of iron oxide nanoparticles has been identified as an alternative route to synthesize Iron Oxide nanoparticles of desired shapes and sizes owing to the relative abundance bio-reductant, ease of preparation, cost effectiveness facileness and benignity. The most extensively acknowledged protocol in the biological synthesis of nanoparticles is the use of plant extracts (Matinise, 2017). Plants with different forms of genetic differences contain a potent array of interesting phytochemical constituents including alkaloids, flavonoids, tannin, saponin, terpenoids, phenols and a host of others which have the potential to reduce metal ions to lower oxidation states in a single step (Suganya *et al.*, 2016). In addition, the synthesis procedure can be carried out at low temperatures and pressures without any cumbersome procedure and easy to optimize. Plants metabolites are advantageous as they serve excellent reducing, stabilizing and capping agents, therefore circumventing the use of toxic chemicals as reducing agents (Shanker *et al.*, 2016). Hence, the present study focuses on the synthesis of iron oxide nanoparticles using the leaf extract of *Calotropis procera* as bio-reductant and capping agent.

Materials and Method

Materials

Ferric chloride hexahydrate ($FeCl_3.6H_2O$), ferrous sulphate heptahydrate ($FeSO4{\cdot}7H_2O$), hydrochloric acid (HCl) and sodium hydroxide (NaOH), all from

Sigma-Aldrich were used as received. Deionized water was used in the preparation of all solutions.

Preparation of Calotropis procera leaves extract

The leaves of *Calotropis procera* were collected, washed thoroughly with tap water followed by sterile distilled water and air dried under shade for 14-15 days. Dried leaves were incised into small pieces, pulverized using mortar and pestle, and the powdered sample was stored in an air tight container. Ten grams (10 g) of the powdered leaves were weighed into a 250 cm^3 round bottom flask containing 100 cm^3 of distilled water to obtain 0.1 g/cm^3 concentration. This was blended and heated to reflux for thirty minutes at 70 °C until the watery colour of the solution turned yellowish-brown. The extract was cooled to room temperature and strained using a muslin cloth and later filtered using Whatman No. 1 filter paper. The obtained filtrate was poured into a bottle and preserved in a refrigerator at 4°C for subsequent use.

Synthesis of iron oxide nanoparticles

About 30 cm^3 of 0.1 g/cm^3 of aqueous leaves extract *of Calotropis procera* was measured into a conical flask and heated to about 40 °C for about 20 minutes. This extract was later dripped slowly into a conical flask containing 70 cm^3 mixture of aqueous solution of 0.03 M $FeCl_3.6H_2O$ and 0.02 M $FeSO4.7H_20$ on a magnetic stirrer with continuous stirring at 200 rpm and 40 °C for 1 hour. The pH of the solution was adjusted to 9.0 by the dropwise addition of 1 M NaOH and 1 M HCl using calibrated pH meter (Hanna Instruments; Germany). The addition of the aqueous leaf extract resulted to a change from yellow colour of metallic precursor solution to greenish-black colour. The colloidal solution obtained was characterized to confirm the formation of iron oxide nanoparticles, washed repeatedly with distilled water followed by centrifugation at 2,500 rpm for 2 minutes after each stage of washing until a neutral pH was obtained which aided the removal of the residual by-products. The purified nanoparticle was later oven dried at 60 °C overnight and stored in an airtight container.

Characterization of the prepared nanoparticles

The absorbance spectra of sample were measured with the help of Shimadzu Ultraviolet- Spectrophotometer (UV-1800, 240v) within the range of 200-700 nm wavelengths. The average size of the green synthesized iron oxide nanoparticles was observed using zeta sizer dynamic light scattering (Zen 1600, UK). The phase structure of the synthesized iron oxide nanoparticles was examined by X-ray diffraction technique using Rigaku miniflex 600 with monochromatic copper (Cu)

Kα radiation (λ = 1.5406 Å) in the 2θ range of 10 - 90°, a step size of 0.020° and operating at 40 kV and 15 mA was used. The functional groups present in the nanoparticles were examined by FT-IR spectroscope (Agilent Cary 630 FTIR spectrometer) within the range of 4000 - 400 cm^{-1}. Raman spectroscopy (ProRaman -L- 785-B1S, USA) was further used to study the vibrational phases of the nanoparticles.

Results and Discussion.

A visible colour change from the yellow colour of Fe^{3+}/Fe^{2+} solution to a greenish-black solution was immediately observed on addition of the extract indicating a bio-reduction of the precursor salt. Bio-precipitation was observed and increased on addition of a few drops of 1M NaOH at a pH of 9.0.

UV-Vis spectroscopic Analysis

Figure 4.1 demonstrates the absorption spectra of the as grown iron oxide NPs. The synthesized iron oxide nanoparticles revealed continuous absorption band within the wavelength range of 200-700 nm with an absorption peak at 404 nm which may be attributed to the formation of magnetite (Fe_3O_4). This absorption band confirms the reaction between *Calotropis procera* extract and Fe^{3+}/Fe^{2+} of the precursor salt solution. This result is in accordance with the findings of Sridhar *et al.*, (2018) on green synthesis of magnetic iron oxide nanoparticle using leaves of *Glycosmis mauritiana* where absorption peak was recorded at 404 nm.

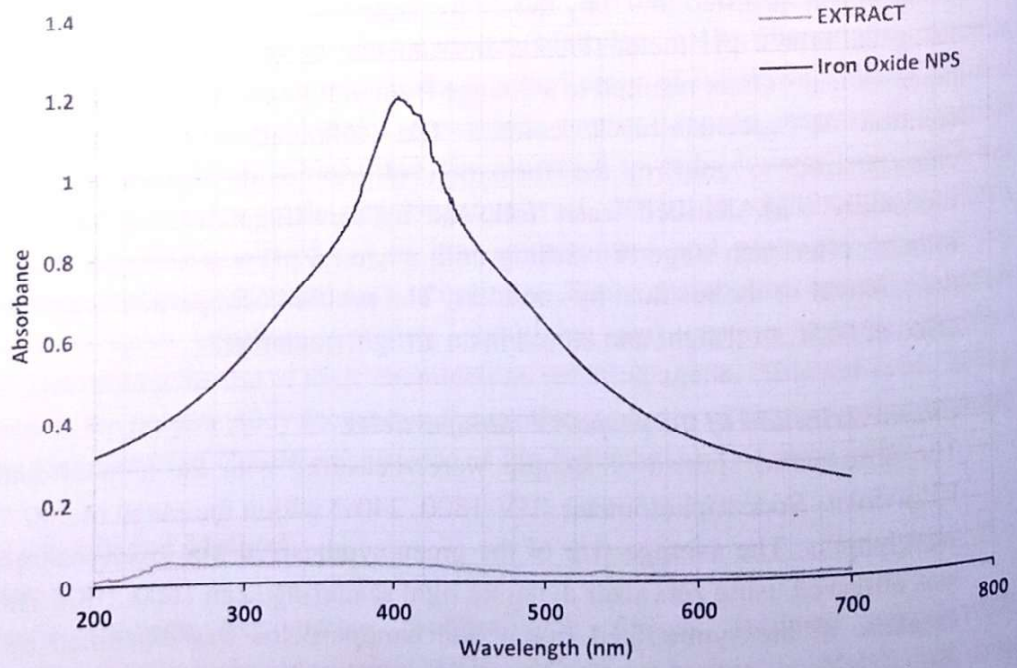

Figure 1: Absorption spectra of iron oxide nanoparticles and leaf extract

Excitation of surface plasmon resonance of the iron oxide nanoparticles induces absorption peak at wavelength between 400-450 nm, which is identical to the characteristic absorption spectrum of iron oxide nanoparticles (Bhavika and Paras, 2017).

DLS Analysis

The DLS revealed an average particle size of 54 nm showing well size reduction by leaf extract of *Calotropis procera*. This result is in agreement with the particle size of 100 nm reported by Kanagasubbulakshmi and Kadirvelu (2017) who used *Lagenaria siceraria* extract in green synthesis of iron oxide NPs.

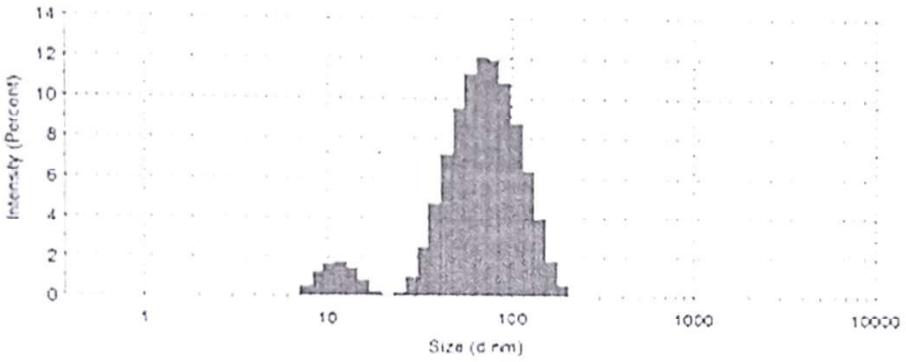

Figure 4.2 Particle Size Distribution of Iron Oxide NPs Analyzed by DLS

XRD Analysis

The XRD pattern displayed the major characteristic peaks for prepared crystalline metallic nanoparticles at 2θ values of 29.99°, 35.6° and 43.12°. The observed diffraction peaks correspond to crystal planes (220), (311) and (400). These peaks depict typical characteristic peak of magnetite (Fe_3O_4) crystal having an inverse cubic spinel structure (Yang *et al.*, 2014) with lattice parameter a = 8.3750 Å, b = 8.3750 Å and c = 8.3750 Å.

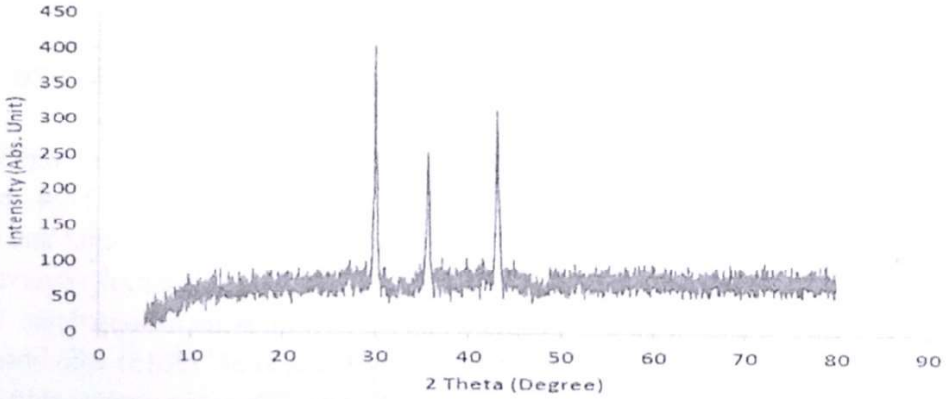

Figure 4.3 X-ray diffractogram of the synthesized iron oxide NPs

The X-ray diffractogram favoured the formation of pure phase magnetite with no mix phase of maghemite nor hematite. This result is in agreement with the outcome of

Venkateswarlu *et al.*, (2014) who found that the iron oxide nanoparticles prepared using $FeCl_3.6H_20$ and *P. Granatum* rind extract were completely pure magnetite phase. The average crystallite size of the iron oxide nanoparticle was calculated to be 19.6 nm using Debye-Scherrer equation which is given by:

$$D = \frac{K\lambda}{\beta Cos\theta}$$

Where K = Constant (0.9), λ = Wavelength of X-ray (1.541 Å), β = FWHM in radians

θ = Diffraction angle in degrees and 10 Å = 1 nm.

Raman Spectroscopy

The Raman spectrometry enabled an easy interpretation and identification of sensitive structures in the prepared iron oxide nanoparticles. The Raman spectrum which revealed the main features of the prepared sample.

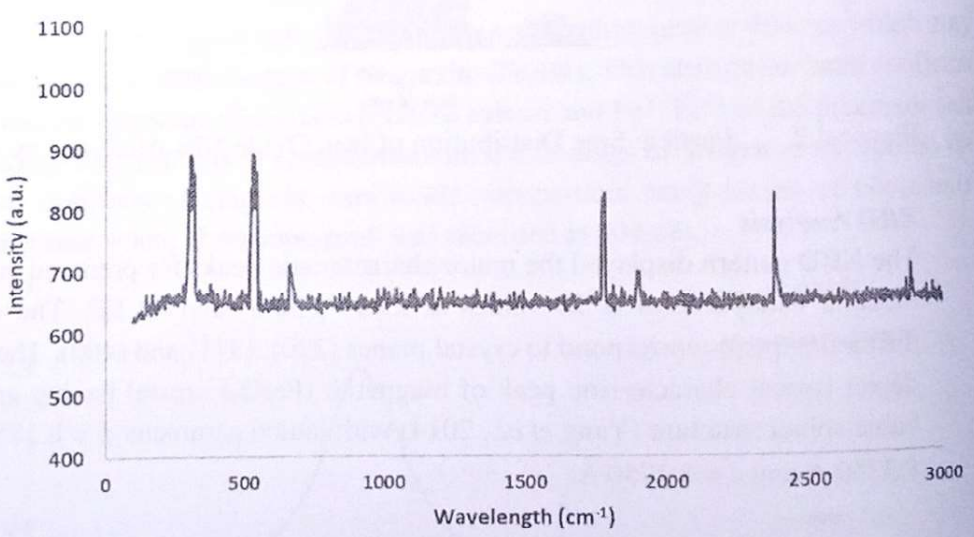

Figure 4 Raman Spectroscopy of the prepared Fe3O4 NPs

From the Raman spectrum, the dominant structures are observed at seven respective wavelengths of about 310 cm^{-1}, 544 cm^{-1}, 668 cm^{-1}, 1174 cm^{-1}, 1908 cm^{-1}, 2390 cm^{-1} and 2876 cm^{-1}. Wavelengths of 310 cm^{-1}, 544 cm^{-1} and 668 cm^{-1} depict Fe-O stretching vibration (Rahman *et al.*, 2011). The peak observed at 668 cm-1 may be attributed to magnetite phase of iron oxide nanoparticles. The peak at 668 cm^{-1} is in line with that obtained by Panta *et al.*, (2015) who observed the peak for magnetite at 670 cm^{-1} using laser 514 nm. The wave number shift observed

at 310 cm^{-1} and 544 cm^{-1} may be as a result of various dimensional effects due to partial oxidation of the particles. These two additional peaks are a representative of vibrational modes corresponding to Fe_3O_4 formation. Similar peaks observed in the work of Gonzalez (2013), according to the author were suggestive of Fe_3O_4 T2g and Eg vibrational modes respectively. The absence of O-H stretching of phenolic groups at wavelengths above 3000 cm^{-1} implies the exclusion of ferric oxyhydroxide from the nanoparticles. Nevertheless, the peaks witnessed at 1174 cm^{-1} and 2876 cm-1 are those of stretching vibration bands of C-H and C-O groups respectively.

FTIR Analysis

Figure 5 shows the FTIR spectra of the synthesized iron oxide nanoparticles. The biomolecules that may be responsible for the reduction of metal precursors and capping agents are identified with stretching vibrations at 3421.8 cm^{-1} and 1660.1 cm^{-1}. The peak at 3421.8 cm^{-1} corresponds to -OH bond stretching of phenolic group while the peak at 1660.1 cm^{-1} indicates the presence of carbonyl groups (-C=O). Similar functional groups were identified in the FTIR spectra of iron oxide nanoparticles synthesized using leaves of *Glycosmis mauritiana* (Amutha and Sridhar, 2018). The formation of magnetite nanoparticles can be attributed to the absorption band at 586 cm^{-1} as a result of Fe-O stretching vibrations.

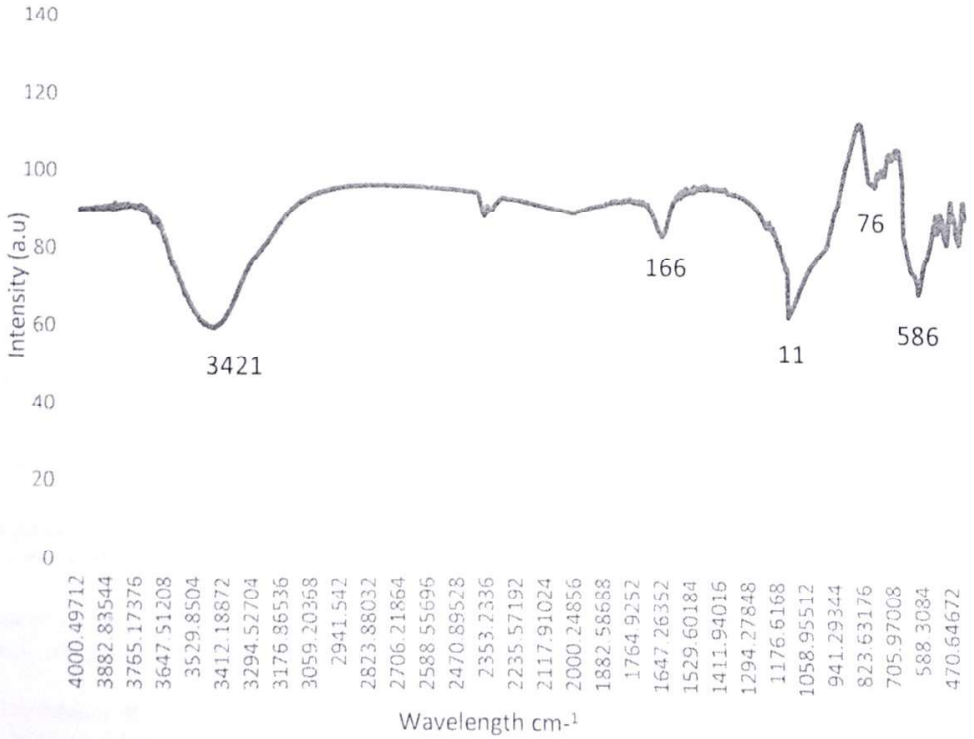

Figure 5 FTIR spectrum of the synthesized iron oxide nanoparticles

Conclusion

In this work, iron oxide nanoparticles have been successfully synthesized via a phyto-enhanced route. The leaf extract of *Calotrois procera* has proved to be a viable biological reductant and capping agent in the production of benign iron oxide nanoparticles. The facile Fe_3O_4 nanoparticle were characterized by UV-Vis, DLS, XRD, Raman spectroscopy and FTIR. XRD revealed typical characteristic peak of Fe_3O_4 crystal having average crystallite size of 19.6 nm with possible potential applications in smart fluids, magnetic resonance imaging, environmental remediation and energy transformation.

References

Bhavika, T., & Paras, T. (2017). Green synthesis of Zero valent iron nanoparticles from *Coriandrum sativum* and its application in reduction chemical oxygen demand and biological oxygen demand in waste water. *South - Asian Journal of Multidisciplinary Studies,* 132-139.

Beheshtkhoo, N., Kouhbanani, M. A., Savardashtaki, A., Amani, A. M., & Taghizadeh, S. (2018). Green synthesis of iron oxide nanoparticles by aqueous leaf extract of Daphne mezereum as a novel dye removing material. Appl. Phys, A-Mater 124(5).

Campos, E. A., Pinto, D. V., Oliveira, J. I., Mattos E.C., & Dutra, R.C., (2015). Synthesis, Characterization and Applications of Iron Oxide Nanoparticles – a Short Review. J. Aerosp. Technol. Manag., 7(3), 267-27

Gonzalez, J. P. (2013). Synthesis and characterization of iron oxide thin films for use in electrical devices. M.Sc. Thesis, Submitted to Department of Chemistry, San Diego State University, California. Pp. 32-34.

Kanagasubbulakshmi, S., & Kadirvelu, K. (2017). Green Synthesis of Iron Oxide Nanoparticles using *Lagenaria Siceraria* and Evaluation of its Antimicrobial Activity. Defence Life Science Journal, 2(4), 422-427, DOI: 10.14429/dlsj.2.12277

Mandeep, K., & Dimple, S. C. (2018). Green Synthesis of Iron Nanoparticles for Biomedical Applications. Glob J Nano. 4(4): 555643. DOI: 10.19080/GJN.2018.04.555643

Mahmoud, O., Nasr El-Din, H., Vryzas, Z., & Kelessidis, V. (2016). Nanoparticle Based Drilling Fluids for Minimizing Formation Damage in HP/HT Applications. SPE International Conference and Exhibition on Formation Damage and Control (pp. 1-26). Louisiana: Society of Petroleum Engineers.

Matinise, N. (2017). Zinc oxide nanoparticles via *Moringa oleifera* green synthesis: Physical properties and mechanism of formation. Applied Surface Science, 406, 339-347.

Panta, P. C., & Bergmann, C. P. (2015). Raman Spectroscopy of Iron Oxide of Nanoparticles (Fe3O4). J Material Sci Eng 5: 217. doi:10.4172/2169-0022.1000217

Rahman, M. M., Khan, S. B., Jamal, A., Faisal, M., & Aisiri, A. M. (2011). Iron Oxide Nanoparticles. In Rahman, M. (Ed.), Nanomaterials (pp. 50-53) ISBN: 978-953-307-913-4.

Saif. S., Tahir, A., & Chen, Y., (2016). Green Synthesis of Iron Nanoparticles and Their Environmental Applications and Implications. Nanomaterials 2016, 6, 209; doi:10.3390/nano6110209

Shanker, U., Jassal, V.,Rani, M., & Kaith, B. S. (2016). Towards green synthesis of nanoparticles: from bio-assisted sources to benign solvents. A review. Int. J. Environ. Anal. Chem. 96 (9), 801-835. http://dx.org/10.1080/03067319.2016.1209663

Sridhar, S., & Amutha, S. (2018). Green synthesis of magnetic iron oxide nanoparticle using leaves of *Glycosmis mauritiana* and their antibacterial activity against human pathogens. Journal of Innovations in Pharmaceutical and Biological Sciences, 5(2), 22-26

Suganya, D., Rajan, M. R., & Ramesh, R. (2016). Green synthesis of iron oxide nanoparticles from leaf extract of *Passiflora foetida* and its antibacterial activity. International Journal of Current Research, 8 (11): 4208142085.

Venekateswarlu, S., & Yoon, M. (2015). Rapid removal of cadmium ions using green-synthesized Fe3O4 nanoparticles capped with diethyl-4-(4amino-5-mercapto-4H-1,2,4-triazol-3-yl) phenyl phosphonate. RSC Adv. 5, 65444- 65453.

Yang, D., Pang, X., He, Y., Wang, Y., Chen, G., Wang, W., & Lin, Z. (2015). Precisely size-tunable magnetic/plasmonic core/shell nanoparticles with controlled optical properties. Agnew. Chem. Int. Ed. 54: 12091-12096. doi:http://dx.doi.org/10.1002/anie.201504676

Yew, Y. P., Shameli, K., Miyake, M., Kuwano, N., Khairudin, N. B., Mohamad, S. E., & Lee, K. X. (2016). Green Synthesis of Magnetite (Fe3O4) Nanoparticles Using Seaweed (*Kappaphycus alvarezii*) Extract. Nanoscale Research Letters, 11:276